Cellulose/Poly(4-vinylpyridine) Blends

Jean-François Masson† and R. St. John Manley*

Pulp and Paper Research Centre and Department of Chemistry, McGill University, 3420 University Street, Montreal, Quebec, Canada H3A 2A7

Received April 9, 1991

ABSTRACT: The miscibility behavior of cellulose (CELL) with poly(4-vinylpyridine) (P_4VPy) was compared to that of the methylolcellulose/P_4VPy pair (MC/P_4VPy). The homopolymers and their blends were characterized by dynamic mechanical analysis (DMA), CP-MAS NMR spectroscopy, and proton spin–lattice relaxation measurements in the rotating frame ($T_{1\rho}$). By fitting the T_g data for the two series of blends to T_g–composition models proposed by Gordon and Taylor and by Jenckel and Heusch, it is shown that the relative strength of the interactions in the CELL/P_4VPy pair is higher than that in the MC/P_4VPy pair; this is confirmed by CP-MAS NMR spectroscopy. The combined results obtained by DMA and proton $T_{1\rho}$ measurements show that MC and P_4VPy are miscible on a scale between 2.5 and 15 nm, while the CELL/P_4VPy pair is probably miscible on a scale of 2.5 nm.

Introduction

For two polymers to be miscible, favorable intermolecular interactions must occur between them. Cellulose, which contains three hydroxyl groups per repeating unit, has the potential to interact with synthetic polymers that can form hydrogen bonds; therefore polyamides, polyesters, and many vinyl polymers would be expected to be miscible with cellulose. Notwithstanding, other factors must influence the miscibility of synthetic polymers with cellulose because nylon-6 has been shown to be immiscible and poly(ε-caprolactone) was shown to be only partially miscible.[1] These two polymers tend to self-associate and it is thus highly probable that this factor impedes their miscibility with polymers like cellulose, which would a priori be expected to interact strongly with them.

It is with this in mind that we recently investigated miscibility in blends of cellulose and poly(vinylpyrrolidone) (PVP).[2] The latter possesses a tertiary amide group, which can interact with the cellulose hydroxyls, in addition to being amorphous so that complications due to crystallization in the blends cannot arise. We believe that it is precisely for this reason that PVP is miscible with cellulose over the whole composition range as we have shown,[2] in contrast to certain other cellulose/synthetic polymer blends.[1,3] It is interesting to note that poly(4-vinylpyridine) (P_4VPy) has the same characteristics as PVP; it is amorphous and possesses a functionality that can interact strongly with cellulose. Thus, it is expected that cellulose and P_4VPy should be miscible. The purpose of the present paper is to present the results of a study of the miscibility of this polymer pair.

Blend films covering the entire composition range were prepared by casting from mixed polymer solutions in the solvent dimethyl sulfoxide (DMSO)/paraformaldehyde. In these blend films the cellulose is in the form of a methylol derivative from which the methylol groups can, however, be readily removed by hydrolysis. This has allowed us to compare the miscibility behavior of cellulose/poly(4-vinylpyridine) blends to that of the methylolcellulose/P_4VPy pair. From this we will be able to ascertain whether methylolcellulose can be used as a probe for unmodified cellulose in blends with synthetic polymers. The state of miscibility of the blend pairs was investigated by measuring the glass transition temperature (T_g) by means of dynamic mechanical testing[4,5] while with NMR spectroscopy, we looked for specific interactions between the polymer moieties. Finally, we estimated the domain size produced upon blending by spin-diffusion measurements.[2,6-8]

Experimental Section

Materials. The cellulose used in this study has been described elsewhere.[2] Poly(4-vinylpyridine), with a nominal viscosity-average molecular weight of 200 000 (Reilline 4200 Powder—Developmental Product), was kindly supplied by Reilly Tar & Chemical Corp.; the sample was purified by dissolution in methanol and precipitation in ethyl acetate and dried before it was used. Dimethyl sulfoxide (HPLC grade, catalog no. 27,043-1) and paraformaldehyde (catalog no. 15,812-7), both purchased from Aldrich Chemical Co., were used as supplied.

Preparation of Samples. The dissolution of cellulose in DMSO via formation of its methylol derivative was originally described by Johnson et al.[9] A modification of this procedure was used to obtain the 1.45% cellulose solution used in this study. We have described the modification of the original procedure in a recent paper.[2] P_4VPy was dissolved in DMSO at room temperature to give a 4.5% solution. The cellulose and P_4VPy solutions were mixed in appropriate ratios to produce blends with composition ranging from 10/90 to 90/10 (w/w), the first number referring to cellulose throughout this work. Blend films were cast from the blend solutions in polypropylene dishes in vacuo at room temperature over a period of 24 h. In a first series of blends, the cast films were dried at 125 °C overnight in vacuo, while in a second series of samples the cast films were steeped in a 0.02 N ammonium hydroxide solution, washed in water, and dried in vacuo overnight at 125 °C.

Measurements. The experimental conditions used for the dynamic mechanical analysis, CP-MAS NMR spectroscopy, and proton spin–lattice relaxation measurements have all been described elsewhere.[2]

Results and Discussion

Preliminary Remarks. The homopolymer solutions and the blend solutions were all optically clear and showed no biphasic structures or any precipitation even after 6 months of standing at room temperature. Similarly, the cast homopolymer films and blend films were clear and showed no phase separation that could be perceived with an optical microscope. We have shown[2] that a film of cellulose cast from a methylolcellulose solution in DMSO is actually a methylolcellulose/DMSO complex with a low degree of methylol substitution. After heat treatment at 125 °C for ca. 15 h, the DMSO content of the cellulose was 0.28 (mol/mol), while the degree of substitution was 0.07.

* To whom correspondence should be addressed.
† Present address: National Research Council of Canada, Institute for Research in Construction, Ottawa, ON, Canada K1A 0R6.

0024-9297/91/2224-5914$02.50/0 © 1991 American Chemical Society

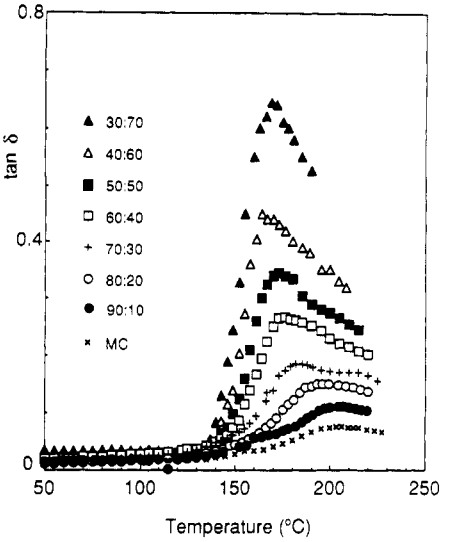

Figure 1. tan δ temperature dependence of MC and MC/P_4VPy blends. Curves for pure P_4VPy, the 10:90 blend, and the 20:80 blend are not shown. See text for details.

Thus, strictly speaking, the cast heat-treated cellulose film is a methylolcellulose/DMSO film. For convenience, throughout the remainder of this paper the cast heat-treated cellulose will be termed methylolcellulose because of its methylol content and will be abbreviated as MC. Hence from casting, solid films of MC/P_4VPy blends are obtained. A second series of blends is obtained from the hydrolysis of the methylol adducts that remained on MC after heat treatment and removal of the bound DMSO, with an ammonium hydroxide solution, to give cellulose (CELL)/P_4VPy blends. The physical aspect of this second series of blend films is like that of the first series of films (MC/P_4VPy) and could not be differentiated from it by visual means.

Dynamic Mechanical Analysis (DMA). In previous studies[1-3,10] it was shown that by means of DMA an assessment of the extent of mixing between cellulose and synthetic polymers is facilitated because of the higher sensitivity of the method compared to differential scanning calorimetry (DSC). From DMA three parameters are obtained as a function of temperature: the loss tangent tan δ, the loss modulus E'', and the storage modulus E'. In the T_g region a maximum appears in each of the tan δ and E'' vs temperature spectra, while there is a decrease in the storage modulus (E') due to a loss in stiffness, so that a plot of E' vs temperature reveals an important drop. Consequently, the three parameters that can be measured by DMA, the loss tangent tan δ, the loss modulus E'', and the storage modulus E', can be used to determine T_g albeit E' and E'' usually produce the same value for T_g. These parameters are sensitive to many processes,[4] including structural heterogeneities and molecular motions, so that changes in the immediate environment of a given polymer chain caused by intimate mixing can be recognized from a change in the position of the tan δ or E'' maxima or the midpoint in the drop of E'.

The results of the DMA study on the MC/P_4VPy and CELL/P_4VPy blends are shown in Figures 1–4. For reasons already discussed,[2] for blends with a high amorphous synthetic polymer content, in this instance P_4VPy, it is not possible to obtain a complete tan δ curve with the use of the Rheovibron viscoelastometer;[2] thus the tan δ maxima are not observed for P_4VPy, the 10:90 and 20:80 MC/P_4VPy blends, and the 10:90 and 20:80 CELL/P_4VPy blends. The precise location of the tan δ maximum related to T_g for pure P_4VPy was obtained from a heat-

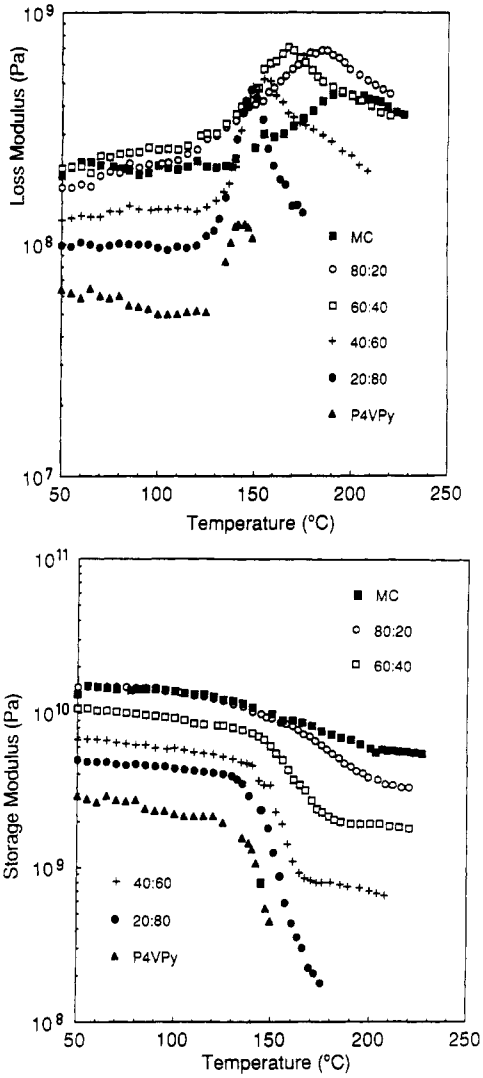

Figure 2. (Top (a)) Loss modulus (E'') temperature dependence of P_4VPy, MC, and some of their blends. The other blends were omitted for clarity of presentation. (Bottom (b)) Storage modulus (E') temperature dependence of P_4VPy, MC, and some of their blends. The other blends were omitted for clarity of presentation.

pressed sample run on a dynamic mechanical thermal analyzer under conditions already described.[2]

The tan δ temperature dependence of MC shows a low-intensity peak at 208 °C (Figure 1). In a recent paper[2] we hypothesized that this T_g arises from the presence of both DMSO and the methylol substituents, which depress the T_g of pure cellulose from its estimated value of ca. 250 °C.[3,11] However, the degree of substitution (DS) of MC was then 0.78 whereas in the present case it is 0.07, thus roughly 10 times lower because of longer drying time (the DMSO content remained the same). Despite the fact that the T_g of cellulose depends on its DS,[11] the T_g of MC remains constant at 208 °C. It would thus appear that the DMSO content being larger than the methylol adduct content, in terms of weight percent, the DS becomes insignificant as far as its effect on T_g is concerned. P_4VPy, on the other hand, shows a single peak corresponding to its T_g centered at 169 °C (not shown), in contrast to the thermally stimulated discharge (TSD) spectrum of P_4VPy, which shows two transitions above room temperature:[12] an α transition at 157 °C associated with T_g, where motions of the chains in the amorphous regions become indirectly evident, and a β transition at 117 °C believed to arise from torsional motions of the pyridine ring. The absence of the β transition in the DMA spectrum of P_4-

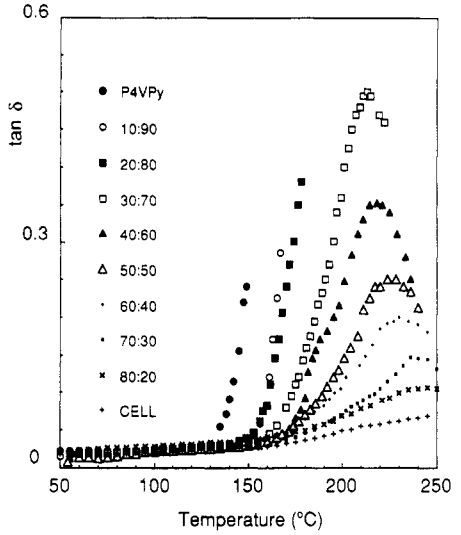

Figure 3. tan δ temperature dependence of CELL, P_4VPy, and their blends.

VPy should not be surprising since it originates from an internal polarization effect that can be measured only by means of electrical methods like TSD. The difference in the mechanism giving rise to T_g probably accounts for the different T_g temperatures recorded by the DMA and TSD methods.

Blending P_4VPy with 10, 20, 30, or 40% MC does not have any effect on the position of the observed tan δ peaks for the blends, apart from a reduction in intensity due to a decreasing P_4VPy content in the blend. The measured peak position for these blends is 169 °C, the same temperature as for unblended P_4VPy. This transition must therefore arise only from the P_4VPy portion of the blend, while the high-temperature MC peak is too low in intensity to be observed. Accordingly, on the basis of these tan δ measurements, MC and P_4VPy appear to be immiscible in the composition range 10/90 to 40/60. As the blend composition is changed to 50/50, the recorded tan δ peak of the blend moves to a slightly higher temperature of 173 °C. This modest increase in T_g nonetheless indicates some mixing between MC and P_4VPy. As the composition of the blend is increased beyond 50/50, the T_g increases conspicuously as apparent from the tan δ maxima in the curves of the 60/40 to 90/10 blends (Figure 1), although the magnitude of the transition keeps decreasing proportionally with the content of MC in the blend. The 60/40 blend thus displays a tan δ peak, corresponding to T_g, at 176 °C, the 70:30 blend at 185 °C, the 80:20 blend at 196 °C, and the 90:10 blend at 204 °C. This suggests that in blends containing 50% MC or more the two polymers are miscible.

Panels a and b of Figure 2 show respectively the loss modulus (E'') and the storage modulus (E') temperature dependence of the MC/P_4VPy blends. The E'' relaxation of MC is located at 208 °C, the same temperature as the tan δ peak; however, it is more clearly distinguishable than the tan δ peak. P_4VPy, on the other hand, shows the E'' relaxation related to T_g at 145 °C, a much lower temperature than the tan δ relaxation. Such a large difference in temperature between the tan δ and E'' peaks has also been observed for polyacrylonitrile,[3] poly(vinylpyrrolidone),[4] and poly(acrylic acid).[13] This phenomenon appears to be common to synthetic polymers possessing a large amorphous content. It is interesting to note that the general behavior displayed by the moduli of the blends is different from that displayed by tan δ. As was the case for the tan δ behavior of the 10:90 blend, the peak in E''

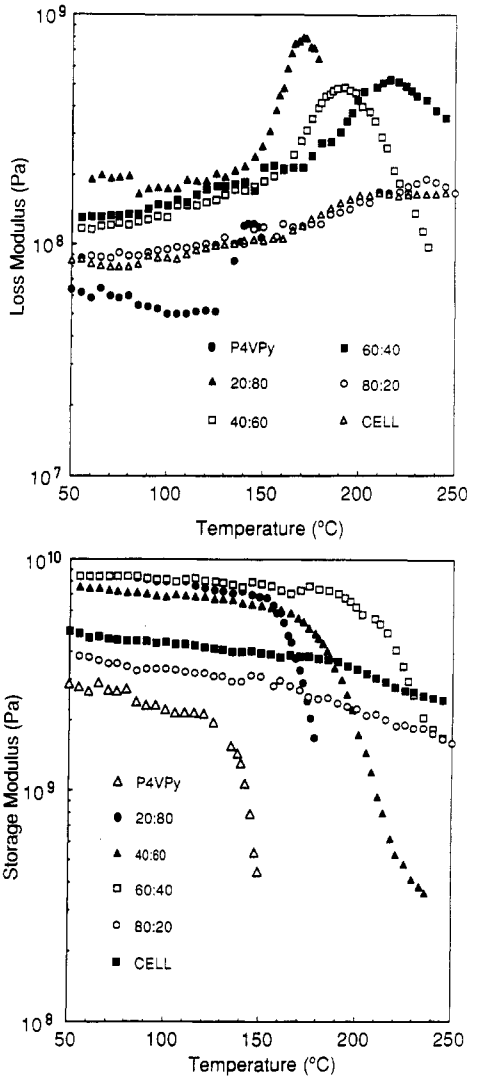

Figure 4. (Top (a)) Loss modulus (E'') temperature dependence of P_4VPy, CELL, and some of their blends. The other blends were omitted for clarity of presentation. (Bottom (b)) Storage modulus (E') temperature dependence of P_4VPy, CELL, and some of their blends. The other blends were omitted for clarity of presentation. Note that the curves for the P_4VPy and 20:80 blends are incomplete because measurements at higher temperature could not be performed (see text for details).

and the drop in E' occur at the same temperature as for the unblended P_4VPy. However, in contrast to the tan δ behavior, as soon as the content of the blend reaches 20:80, an increase in T_g is observed, so that the E'' peak and E' slope appear at ca. 148 °C. From this composition up to 100% MC the position of the E'' transition and the midpoint in the decrease in E' appear at a higher temperature with successive changes in composition. The position of the E'' peaks and the tan δ values obtained at each MC/P_4VPy composition are shown in Table I. The trend of the E'' values, in contrast to that shown by the tan δ values, reveals miscibility essentially over the whole composition range. Thus, the temperature at which the E'' transition appears increases as the composition is varied from unblended P_4VPy to unblended MC, and at every blend composition a single transition is observed. It has been noted that E'' is a more sensitive indicator of molecular order than tan δ.[14] Similarly from the data of tan δ and E'' on MC/P_4VPy blends it would appear that E'' is also more sensitive than tan δ to changes in the immediate environment of the polymer chains caused by blending.

As we go from MC to CELL, the T_g goes from 208 to 250 °C, so that it is easier to see the shifts in T_g's for the

Table I
T_g As Obtained from the tan δ and E'' Peaks for MC, CELL, P_4VPy, and Their Blends

	MC/P_4VPy		CELL/P_4VPy	
blend comp[a]	tan δ	E''	tan δ	E''
0/100	169	145	169	145
10/90	169[b]	145	ND[c]	160
20/80	169[b]	148	ND	170
30/70	169	152	213	183
40/60	169	155	218	190
50/50	173	158	224	200
60/40	176	167	230	216
70/30	185	173	236	223
80/20	196	184	240	235
90/10	204	194	ND	ND
100/0	208	208	250[d]	250[d]

[a] Weight ratio. [b] Estimated. [c] Not determined. [d] Expected value, refs 3 and 11.

CELL/P_4VPy blends in comparison with the T_g shifts for the MC/P_4VPy blends, as shown in Figures 3 and 4. Unlike the tan δ temperature dependence of the MC/P_4VPy blends, the temperature onset of the tan δ transition for the CELL/P_4VPy blends moves to the high-temperature side as the cellulose content in the blend is increased. This is most marked as the composition changes from pure P_4VPy, which shows an onset in its tan δ transition at ca. 135 °C, to the 10:90 or 20:80 blends, which show an onset in their tan δ curve at ca. 155 °C. The onset of the transition of the 30:70 blend is still higher at ca. 165 °C, and it continues to move up as the cellulose content in the blend is increased; simultaneously it becomes less conspicuous because of the decreasing intensity in the tan δ transition. Although for pure P_4VPy and the 10:90 and 20:80 CELL/P_4VPy blends the maxima in the tan δ curve are not observed, for reasons explained previously, it is easy to imagine that they would appear at an increasingly high temperature, first because of the relatively low temperature transition onset for P_4VPy and second because the slope of the rising portion of the 10:90 and 20:80 blends is different and would necessarily lead to a maximum located at a different temperature. When the CELL/P_4-VPy blend composition reaches 30:70, the maximum of the tan δ transition, centered at 213 °C, becomes clear. As the CELL content in the blend progressively increases, the center of the tan δ peak moves to still higher temperatures and similar to the MC/P_4VPy blends the height of the transition progressively dimishes. In contrast to the latter, however, the tan δ behavior of the CELL/P_4-VPy blends shows that the two polymers are practically miscible over the whole composition range and not only at compositions with 50% cellulose or more.

In accordance with the tan δ temperature dependence of the blends, the moduli temperature dependences, E'' and E', show clearly that CELL and P_4VPy are miscible. For example, P_4VPy shows a maximum in its E'' spectrum (Figure 4a) and a drop in its E' spectrum (Figure 4b) at a temperature of 145 °C while the 20:80 blend shows an E'' peak centered at 170 °C and a drop in E' at the same temperature. The E'' peak for the 40:60 blend and the slide in E' appear at a still higher temperature, 190 and 200 °C, respectively. As the cellulose content in the blend further increases the T_g, which manifests itself with the appearance of a peak in the E'' spectrum and a slide in the E' spectrum, moves to increasingly higher temperatures. In none of the blends is there the appearance of a shoulder to these maxima, and likewise no breaks or plateaus in the drop of E' reveal any sign of incomplete mixing between CELL and P_4VPy. The peak maxima for tan δ and E'' for the whole series of CELL/P_4VPy blends are shown in Table I. The increase in T_g for these blends as the composition is varied from pure P_4VPy to pure CELL is characteristic of a polymer blend pair that is miscible, and since DMA reveals a single T_g in polymeric mixtures with domain sizes smaller than ca. 15 nm,[15] CELL and P_4VPy must therefore blend on a comparable scale, if not better, as we will see later.

Although the moduli responses of both blend pairs, MC/P_4VPy and CELL/P_4VPy, show that the two pairs form miscible polymer blends, it is interesting to note that from the comparison of the tan δ response of the two blend systems it would appear that the MC and P_4VPy do not blend as well as do CELL and P_4VPy. In the former pair the tan δ relaxation response is independent of composition below 50% MC. Such behavior is typical of immiscible blend pairs. On the other hand, in the latter pair, in the same concentration range tan δ varies in a manner that is expected of miscible blends. Consequently, CELL and P_4VPy must blend on a smaller scale than do MC and P_4VPy. As we will see in the next section, this conclusion is supported by the difference in the relative strength of interaction between the components in the MC/P_4VPy and CELL/P_4VPy blends.

T_g–Composition Relationships. Several semiempirical equations have been used to model the variation of T_g as a function of blend composition.[16-23] Among these, three equations contain a parameter that can be related to the strength of interaction between the constituent polymers of the blends. From the calculation of these parameters it is possible to compare the relative strength of interaction between the constituent polymers of the MC/P_4VPy and CELL/P_4VPy blend pairs.

To explain the lowering of T_g by plasticizers Jenckel and Heusch proposed the expression[24]

$$T_g = W_1T_{g1} + W_2T_{g2} + W_1W_2b(T_{g1} - T_{g2}) \quad (1)$$

where W_i and T_{gi} are the weight fraction and glass transition temperature of the respective polymers. The constant b originally characterized the efficiency of the plasticizer to depress the T_g of the pure polymer, i.e., the interaction between the plasticizer and the polymer. Such a reasoning can very well be applied to characterize polymer blends. The constant b then becomes a measure of how well two polymers interact with one another, b being inversely proportional to the strength of interaction between the polymers.[22,23]

Similarly, Gordon and Taylor proposed the expression[25]

$$T_g = (W_1T_{g1} + kW_2T_{g2})/(W_1 + kW_2) \quad (2)$$

to predict the T_g behavior of binary random copolymers, the constant k being defined as $\Delta\beta_2/\Delta\beta_1$, where β_i is the cubic expansion coefficient of component i. The equation was subsequently used to explain the T_g–composition dependence of polymer blends, with k proportional to the strength of interchain interaction.[17,22,23]

Later Kwei proposed a modification to the Gordon–Taylor equation to account for hydrogen bonding between the blend components:[19]

$$T_g = (W_1T_{g1} + kW_2T_{g2})/(W_1 + kW_2) + qW_1W_2 \quad (3)$$

where the qW_1W_2 term can be taken as the contribution of hydrogen bonds, with q proportional to the strength of the hydrogen bond. When $k = 1$ this equation is identical with the Jenckel–Heusch equation with $q = b(T_{g1} - T_{g2})$. The k value of the Gordon–Taylor equation, the b value of the Jenckel–Heusch equation, and the q value of the Kwei equation have all been used to compare the strength of interchain interaction in blend systems.[17,22,23]

Table II
Parameters in the Gordon–Taylor, Jenckel–Heusch, and Kwei Equations Used To Compare the Strength of Interactions in the Miscible Blend Systems[a]

blend system	Gordon–Taylor k	Jenckel–Heusch b	Kwei k	Kwei q
MC/P_4VPy	0.28	1.10	0.48	−23.00
CELL/P_4VPy	1.27	−0.23	1.00	21.85

[a] Calculated from a standard least-squares procedure to obtain the best fit of the loss modulus data.

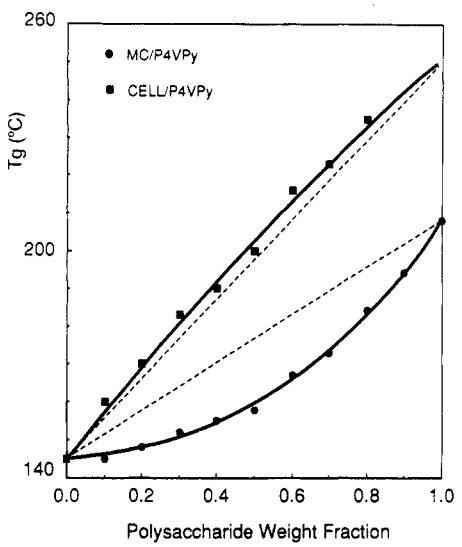

Figure 5. Theoretical T_g of MC/P_4VPy and CELL/P_4VPy blends as a function of composition (full line), calculated to give the best fit to the E'' data points. The broken line is the tie line representing the weight-average values. Note that the T_g of CELL was not actually measured; the estimated value of 250 °C was used for the calculations.

In Table II we show the parameter values obtained with the various equations, as calculated from least-squares procedures to obtain the best fit to the T_g experimental data, using the loss modulus (E'') of both the MC/P_4VPy and CELL/P_4VPy blends. The T_g values as obtained from tan δ were not modeled because of the behavior characteristic of immiscible blends (MC/P_4VPy) or because of an incomplete data set (CELL/P_4VPy). The T_g values predicted by the Gordon–Taylor, Jenckel–Heusch, and Kwei equations for the MC/P_4VPy and CELL/P_4VPy blends fit the experimental data satisfactorily. As an example, in Figure 5 are shown the T_g values calculated with Kwei's model. The curves for the Gordon–Taylor and Jenckel–Heusch models were omitted for clarity of presentation. The curve-fitting procedures of the CELL/P_4VPy data by the Jenckel–Heusch and Kwei equations are indistinguishable from one another since $k = 1$ in that case. The predictions of the Gordon–Taylor model for the same data set are so close to those of the other two models that a graph does not reveal the difference in the predicted T_g's. Consequently, all three models are represented by a single curve.

As seen in Figure 5, the T_g results for the MC/P_4VPy blend pair are different from those of the CELL/P_4VPy pair. For MC/P_4VPy the T_g of the blends falls below the calculated weight-average values of the T_g's of the components (negative deviation), while for CELL/P_4VPy the T_g of the blends is higher than the corresponding weight-average values (positive deviation). In previous blend studies[17,18] deviations of the T_g–composition curve from the weight-average values have been related to the strength of the interaction between the blend components. Large

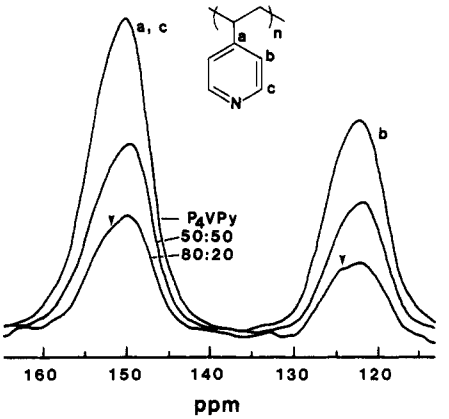

Figure 6. Low-field portion of ^{13}C CP-MAS NMR spectra for P_4VPy in its pure state and in two MC/P_4VPy blends. The labeled peaks correspond to those carbons identified in the structure of P_4VPy.

negative deviations are associated with weak interactions and correspond to low values of k in the Gordon–Taylor equation or high b values in the Jenckel–Heusch equation. On the other hand, a positive deviation has been interpreted as an indication of very strong interactions.[19,20]

In the present study, the trends revealed by the k, b, and q values in the Gordon–Taylor, Jenckel–Heusch, and Kwei equations, respectively (Table II), suggest that the CELL/P_4VPy pair interacts more strongly than the MC/P_4VPy pair. Because stronger interactions lead to better miscibility (unless the number of such interactions is reduced), the evidence for a stronger interaction in the CELL/P_4VPy blends compared to the MC/P_4VPy blends supports our previous assessment, based on the results of the tan δ measurements, that mixing in the former blend is better than in the latter. It is rather gratifying to note that the conclusions reached from the comparison of the tan δ measurements and from the modeling of the E'' data for the two blend pairs, namely, MC/P4VPy and CELL/P4VPy, are the same although the approaches are different.

The different miscibility behavior of the MC and CELL blends probably originates from the particular structure and environment of the two polysaccharides. We must bear in mind that MC is in fact a methylolcellulose/DMSO complex. While the presence of methylol groups on the cellulose backbone should not modify the hydrogen-bonding capacity of the chains with an electron donor, the presence of DMSO molecules bound to the cellulose chains, in contrast, can prevent or affect the interaction of the hydroxyl groups of the polysaccharide with the pyridine functionality of P_4VPy. Thus the difference in miscibility of MC and CELL with P_4VPy probably arises from the residual DMSO bound to MC.

NMR Spectroscopy. Recently, we showed that from NMR spectroscopy we could determine which hydroxyl group of the anhydroglucose unit of cellulose is involved in hydrogen bonding with the functionality of a synthetic polymer.[2] In the present study we demonstrate that the lesser miscibility between the MC and P_4VPy compared to CELL and P_4VPy is due to a lower number of interactions.

Figures 6–9 show the relevant portions of the ^{13}C CP-MAS spectra for CELL, MC, P_4VPy, and selected blends. The assignment of the resonance peaks for the cellulosics and P_4VPy was performed with the aid of their published NMR spectra.[2,27] Changes in carbon chemical shifts, as well as changes in line shape, are observed when the blend composition is varied. An increase or a decrease in electron density around a given nucleus will induce such changes

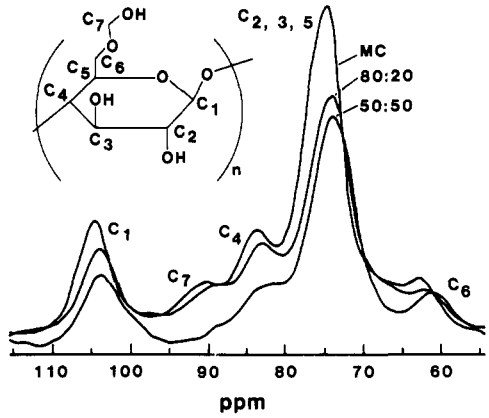

Figure 7. MC portion of ^{13}C CP-MAS NMR spectra for unblended MC and MC/P_4VPy blends. Note that the methylol adduct (C_7OH) can also be on O_2H or O_3H.

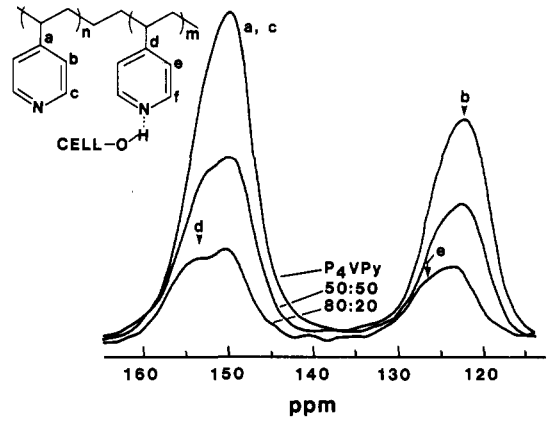

Figure 8. Low-field portion of ^{13}C CP-MAS NMR spectra for P_4VPy in its pure state and in two CELL/P_4VPy blends. The labeled peaks correspond to those carbons identified in the structure of P_4VPy.

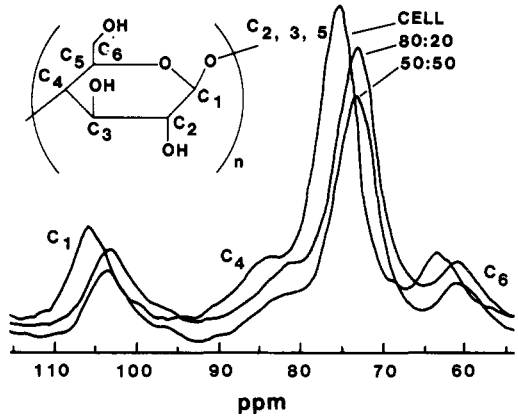

Figure 9. CELL portion of ^{13}C CP-MAS NMR spectra for unblended CELL and CELL/P_4VPy blends.

in isotropic chemical shifts. It is possible to relate a chemical shift to the incidence of hydrogen bonding, since this type of interaction strongly influences the electron density around the carbons bearing the interacting functionalities. Electron densities can also be affected by the proximity of electron-rich or electron-poor functionalities in the vicinity of a given carbon as will become apparent shortly.

The CP-MAS spectrum of P_4VPy displays three peaks. The carbon resonances of the pyridine ring appear at 123.0 and 151.4 ppm (Figure 6), while the resonances of the methylene and methine carbons of the backbone overlap at 40.8 ppm (not shown). Upon blending P_4VPy with MC, the low-field carbon peaks of the P_4VPy moiety at 123.0 and 151.4 ppm do not show changes in line shape or chemical shift unless 80% or more MC is present in the blend. This is seen in the ^{13}C CP-MAS spectrum of the 80:20 blend where a slight but perceptible shoulder appears on the low-field side of both maxima (as shown by the arrows in Figure 6). This change in line shape is nonetheless significant, as we will see later in the analysis of the CELL/P_4VPy blends. Indeed, a chemical shift to the left is a manifestation of a lower electron density, so that this can be readily interpreted as hydrogen bonding of the pyridine ring nitrogen to the available hydroxyl protons of MC. The hydrogen bonding of a proton to the nitrogen of the pyridine ring draws electrons away from the nitrogen, which in turn draws electrons away from the resonance structure of the pyridine ring to compensate for its own decrease in electron density. Therefore the net electron density around the carbon nuclei of the pyridine ring decreases. This gives rise to the observed downfield shift (shift to the left) in the carbon resonance frequencies.

In Figure 7 are displayed the carbon resonances for the MC in its unblended state and in the blends. There are five distinct chemical shifts that correspond to the seven types of carbons found in the MC anhydroglucose (AHG) unit. When MC is blended with P_4VPy, there is an upfield shift (to the right) of all the carbon resonances, reflecting the increase in electron density around the carbons of the AHG unit. The carbons that bear a hydroxyl group (C_2, C_3, C_6, C_7) show a shift in their resonance peak, due to the induced electron-withdrawing effect caused by the interaction of the hydrogen of their respective hydroxyl groups with the nitrogen of the pyridine ring. Even the carbons that are not directly bonded to a hydroxyl group (C_1, C_4, C_5) show a chemical shift, possibly due to the proximity of the electron-rich pyridine rings. In addition, as MC is blended with 50% P_4VPy or more, the resonance peaks of the relatively close C_4 and C_6 carbons are broadened. It is possible that this broadening arises from the superposition of two resonance peaks that are not resolved. In the case of the C_6 resonance peak, one of these unresolved peaks possibly arises from the C_6 carbons bearing the interacting hydroxyl groups, while the other peak could arise from the C_6 carbons bearing the hydroxyl groups that are not interacting. As for the broadening of the C_4 resonance peak, it could arise from the partial superposition of one peak for the C_4 carbons whose electron density is perturbed by the resonance structure of the close pyridine ring, which is interacting with the hydroxyl group at C_6, and one peak from the C_4 part of the AHG units containing the noninteracting C_6 hydroxyl groups. Thus the observed broadening suggests that the miscibility of the MC/P_4VPy blends, observed from the DMA, is a consequence of the interaction between a fraction only of the functional groups of the respective polymers. If all the hydroxyl groups were interacting, then the whole resonance peak would be shifted upfield, without broadening.

By removing the DMSO from MC, which is assumed to act like a shield, in order to get CELL/P_4VPy blends, we expect a larger proportion of the functional groups of CELL and P_4VPy to interact with one another. This is exactly what happens, as shown in Figures 8 and 9. For example, the P_4VPy portion of the spectrum for the 50:50 CELL/P_4VPy blend shows a shoulder on both the 123.0 and 151.4 ppm peaks as was expected, but this shoulder is more pronounced than in the 80:20 MC/P_4VPy blend. The evidence for the interaction of the P_4VPy moiety is

particularly marked for the 80:20 CELL/P_4VPy blend, as shown in Figure 8. What was a shoulder to the peak at 151.4 ppm in the 50:50 blend is now a distinct maximum so that two peaks are now apparent although they are not resolved. Simultaneously the shoulder on the peak at 123.0 ppm has become clearer. There is thus little doubt that a significantly larger number of pyridine rings are interacting, although still only a fraction of them are involved in hydrogen bonding with CELL, based on an argument similar to the one presented previously. The comparison of the spectra for the 80:20 CELL/P_4VPy blend with those of P_4VPy dissolved in methanol or sulfuric acid,[27] where the strength of hydrogen bonding between the pyridine nitrogen and the proton is different, allows us to ascribe the shoulders on the main peaks to specific carbons of the pyridine ring that are engaged in hydrogen bonding as shown in Figure 8. Hence, the ring carbons in the meta and para positions from the nitrogen and part of the rings that are interacting with cellulose become electron deficient. Consequently, they show a downfield shift and appear as shoulders on the main peaks that arise from the carbons of the noninteracting pyridine rings.

The CELL portion of the CP-MAS spectra for the CELL/P_4VPy blends is shown in Figure 9. In contrast to MC, all the peaks are shifted upfield. Therefore, a larger proportion of the available functionalities must be interacting; otherwise broader peaks, resulting from the suggested partial superposition of the carbon resonances for the interacting and noninteracting hydroxyl groups, would be apparent as is the case for the 50:50 MC/P_4VPy blend. The observed shifts are much larger than those for MC in the MC/P_4VPy blends so that the electron density of all the carbons must be higher. Consequently, the interaction between CELL and P_4VPy must be stronger than between MC and P_4VPy.

We have clearly demonstrated with this CP-MAS study that the number of interactions between CELL and P_4VPy is larger than between MC and P_4VPy and that the interactions in the former blends are stronger than in the latter. These results strongly support the conclusions that were reached on the basis of the dynamic mechanical analysis.

Proton $T_{1\rho}$ Measurements. The protons of an amorphous polymer give rise to a single proton $T_{1\rho}$ that is the average of the $T_{1\rho}$'s of the individual protons. This averaging is caused by the strong dipolar coupling between the protons that permit efficient spin diffusion. The rate of spin diffusion is influenced by short-range order so that the homogeneity of mixing in a polymer blend can be assessed from $T_{1\rho}$ measurements.[2,26,28] For example, the protons of an intimately mixed polymer pair show identical relaxation rates, resulting in a single $T_{1\rho}$ value for both components of the blend. A partially miscible polymer pair or an immiscible one, on the other hand, respectively show either partial averaging of the relaxation rates or no averaging at all, depending on the scale of phase separation. Thus the measurement of proton $T_{1\rho}$ values for the components of a given polymer pair provides information of the scale of mixing at the molecular level.

The proton $T_{1\rho}$ values for MC and P_4VPy in their pure states and in the blends were measured from the decaying carbon signal obtained in an interrupted ^{13}C CP-MAS experiment, where a delay time is introduced between the 90° pulse and the CP. Since the proton $T_{1\rho}$ process follows the simple exponential function $M_t = M_0 \exp(-\tau/T_{1\rho})$, the signal M recorded for the various carbons decays with a time constant equal to the proton $T_{1\rho}$. The slope of a semilogarithmic plot of the signal intensity (M_t) vs delay time (τ) thus yields the proton $T_{1\rho}$ value for the different carbon resonances of MC, P_4VPy, and their blends (Figure 10). The relaxation values reported were obtained from the decaying signal of the peaks at 74.2 and 40.8 ppm in MC and P_4VPy, respectively. The results are shown in Table III along with the value for CELL. The proton $T_{1\rho}$ of MC and P_4VPy are only ca. 2.6 ms apart, but it is still apparent that the relaxation time of MC in the blends is different from the relaxation time in its unblended state. The relaxation time of P_4VPy, however, remains almost constant until there is an excess of MC in the blend. The $T_{1\rho}$ values of the components in each blend are equal within experimental error. The spin diffusion across the mixed domains is thus efficient; this results in essentially identical $T_{1\rho}$ values for the two blend components. At first sight, it would thus seem that all the MC/P_4VPy blends are homogeneous on the scale over which spin diffusion proceeds in the time characterized by $T_{1\rho}$, i.e., ca. 2.5 nm, readily calculated with the equation[2]

$$L \approx T_{1\rho}^{1/2} \tag{4}$$

where L is the scale (in nm) over which spin diffusion proceeds in the time $T_{1\rho}$ (in ms). However, because the $T_{1\rho}$ values of the components in the 20:80 and 50:50 blend are effectively the same as the one for unblended P_4VPy, it is more reasonable to suppose that MC is embedded in a P_4VPy matrix, which does not see its molecular motions (related to $T_{1\rho}$) perturbed by the presence of MC. Such a matrix is necessarily inhomogeneous. It follows that not all the blends are homogeneous on a scale of 2.5 nm. This is supported by certain aspects of the CP-MAS spectra

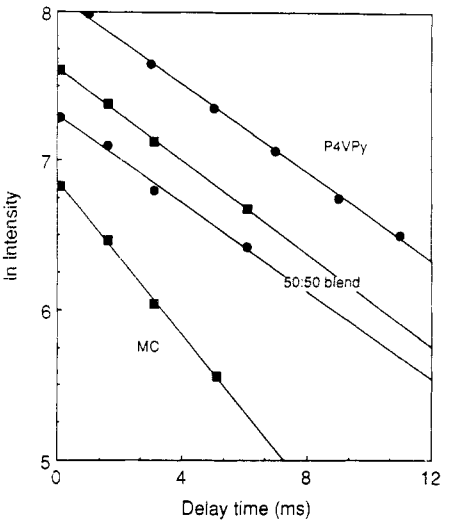

Figure 10. Logarithm of the signal intensity vs delay time for P_4VPy (circles) and MC (squares) in their unblended states and in the 50:50 blend.

Table III
Proton Spin-Lattice Relaxation Time in the Rotating Frame of MC, P_4VPy, and CELL in Their Blended and Unblended States

	$T_{1\rho}$,[a] ms			
system[b]	CELL[c]	MC	P_4PVy	model[d]
0/100			6.8	6.8
20/80		6.6	6.7	6.1
50/50		6.4	6.6	5.2
80/20		5.3	5.9	4.6
100/0		4.2		4.2
100/0	7.5			7.5

[a] ±5%. [b] MC/P_4PVy or CELL/P_4VPy weight ratio. [c] Relaxation times of CELL/P_4VPy blends were not measured. [d] Linear relaxation model.[28,29]

of the three blends studied. Indeed, for changes to be apparent in the CP-MAS spectrum of a blend, the miscibility must be on a scale of the order of 1 nm; otherwise electron densities around carbon nuclei will not be affected. Thus the fact that no changes are apparent in the P_4VPy portion of the CP-MAS spectra of the blends rich in P_4VPy reveals that in these blends the dispersion of MC is poor. Consequently, it appears that the upper limit of homogeneity is 2.5 nm in the MC/P_4VPy blends with less than 50% P_4VPy and that the blends with 50% or more P_4VPy are homogeneous on a scale between 2.5 and 15 nm. The 15-nm upper limit in homogeneity is the one obtained when a single T_g is obtained for a polymer blend.[15]

Although from the $T_{1\rho}$ measurements we could not determine the miscibility of the CELL/P_4VPy pair because the relaxation values of the unblended polymers are equal within the experimental error (Table III), CELL and P_4VPy must mix on a smaller scale than do MC and P_4VPy. This is because the interactions between CELL and P_4VPy are stronger than those between MC and P_4VPy as seen previously and because the number of these interactions seems to be more numerous. Thus CELL and P_4VPy are expected to be homogeneous on a scale of 2.5 nm over the whole composition range.

Concluding Remarks

The present study has shown that CELL and MC are miscible with P_4VPy and that the miscibility persists down to a scale of at least 2.5 nm. It thus appears that MC closely simulates the behavior of cellulose in blends with synthetic polymers. The good state of miscibility in these systems can be readily understood by recognizing that specific chemical interactions can occur between the hydroxyl groups of cellulose (proton donor) and the ring nitrogen of P_4VPy (proton acceptor). As a result strong and numerous hydrogen bonds between the two components can be expected. Chen and Morawetz[30] and Serman et al.[31] have shown that in order to attain miscibility a low density of interacting sites is sometimes sufficient. For the cellulose/P_4VPy system it would be interesting to study how the miscibility of the two polymers changes as the number of interacting sites is reduced. Such an avenue for cellulose polyblend studies has already been suggested in a recent paper.[2] In the present case the use of styrene–4-vinylpyridine copolymers instead of P_4VPy in the cellulose polyblends would allow the study of such an effect.

The cellulose/polymer blend systems studied in recent years have been prepared from either dimethylacetamide–lithium chloride (DMAc–LiCl)[1,3,10,32] or a DMSO–PF^2 system mainly because these two solvent systems do not degrade cellulose to any appreciable extent. However, the availability of only two solvents for the preparation of cellulose/synthetic polymer blends is very limiting. Indeed, several synthetic polymers that could form miscible blends with cellulose, by virtue of their hydrogen-bonding potential, cannot be blended with cellulose because they do not dissolve in DMAc or DMSO. The use of MC as a means to dissolve cellulose and prepare cellulose polyblends, however, may extend the range of solvents that can be employed to prepare these blends. This follows from the fact that MC can also be prepared in tetramethyl sulfoxide, *N*,*N*-dimethylformamide, *N*-methyl-2-pyrrolidinone, and pyridine.[33]

Acknowledgment. J-F.M. thanks Dr. L. A. Belfiore (Colorado State University) for stimulating and helpful discussions and Dr. F. Morin (McGill University) for assistance in performing the NMR experiments. The financial support of the Natural Sciences and Engineering Research Council of Canada, the Fonds pour la Formation de Chercheurs et l'Aide à la Recherche, and the Pulp and Paper Institute of Canada is also acknowledged.

References and Notes

(1) Nishio, Y.; Manley, R. St. J. *Polym. Sci. Eng.* **1990**, *30*, 71.
(2) Masson, J-F.; Manley, R. St. J. *Macromolecules*, in press.
(3) Nishio, Y.; Roy, S. K.; Manley, R. St. J. *Polymer* **1987**, *28*, 1385.
(4) Murayama, T. *Dynamic Mechanical Analysis of Polymeric Material*; Elsevier: Amsterdam, Oxford, New York, 1978.
(5) MacKnight, W. J.; Karasz, F. E.; Fried, J. R. In *Polymer Blends*; Paul, D. R., Newman, S., Eds.; Academic: New York, 1978.
(6) McBrierty, V. J.; Douglass, D. C. *J. Polym. Sci., Macromol. Rev.* **1981**, *16*, 295.
(7) Linder, M.; Hendrichs, P. M.; Hewitt, J. M.; Massa, P. J. *J. Chem. Phys.* **1985**, *82*, 1585.
(8) Parmer, J. F.; Dickenson, L. C.; Chien, J. C. W.; Porter, R. S. *Macromolecules* **1989**, *22*, 1078.
(9) Johnson, D. C.; Nicholson, M. D.; Haig, F. C. *Appl. Polym. Symp.* **1976**, *28*, 931.
(10) Nishio, Y.; Manley, R. St. J. *Macromolecules* **1988**, *21*, 1270.
(11) Kamide, K.; Saito, M. *Polym. J.* **1985**, *17*, 919.
(12) Gable, R. J.; Vijayraghavan, N. V.; Wallace, R. A. *J. Polym. Sci., Polym. Chem. Ed.* **1973**, *11*, 2387.
(13) Nishio, Y., private communication.
(14) McCullough, R. L.; Seferis, J. C. *Appl. Polym. Symp.* **1975**, *27*, 205.
(15) Kaplan, D. S. *J. Appl. Polym. Sci.* **1976**, *20*, 2615.
(16) Aubin, M.; Prud'homme, R. E. *Macromolecules* **1988**, *21*, 2945.
(17) Bélorgey, G.; Prud'homme, R. E. *J. Polym. Sci., Polym. Phys. Ed.* **1982**, *20*, 191.
(18) Bélorgey, G.; Aubin, M.; Prud'homme, R. E. *Polymer* **1982**, *23*, 1053.
(19) Kwei, T. K. *J. Polym. Sci., Polym. Lett.* **1984**, *22*, 307.
(20) Pennacchia, J. R.; Pearce, E. L.; Kwei, T. K.; Bulkin, B. J.; Chen, J.-P. *Macromolecules* **1986**, *19*, 973.
(21) Kwei, T. K.; Pearce, E. M.; Pennacchia, J. R.; Charton, M. *Macromolecules* **1987**, *20*, 1174.
(22) Rodriguez-Parada, J. M.; Percec, V. *Macromolecules* **1986**, *19*, 55.
(23) Pugh, C.; Percec, V. *Macromolecules* **1986**, *19*, 65.
(24) Jenckel, F.; Heusch, R. *Kolloid-Z.* **1953**, *30*, 89.
(25) Gordon, M.; Taylor, J. S. *J. Appl. Chem.* **1952**, *2*, 495.
(26) McBrierty, V. J.; Douglass, D. C.; Kwei, T. K. *Macromolecules* **1978**, *11*, 1265.
(27) Matsuzaki, K.; Matsubara, T.; Kanai, T. *J. Polym. Sci., Polym. Chem. Ed.* **1977**, *15*, 1573.
(28) Dickinson, L. C.; Yang, H.; Chu, C.-W.; Stein, R. S.; Chien, J. C. W. *Macromolecules* **1987**, *20*, 1757.
(29) Douglass, D. C. In *Polymer Characterization by ESR and NMR*; Woodward, A. E., Bovey, F. A., Eds.; ACS Symposium Series 142; American Chemical Society: Washington, DC, 1980.
(30) Chen, C.-T.; Morawetz, H. *Macromolecules* **1989**, *22*, 159.
(31) Serman, C. J.; Xu, Y.; Painter, P. C.; Coleman, M. M. *Macromolecules* **1989**, *22*, 2015.
(32) Nishio, Y.; Hirose, N.; Takahashi, T. *Polym. J.* **1989**, *21*, 347.
(33) Baker, T. J.; Schroeder, L. R.; Johnson, D. C. *Cellulose Chem. Technol.* **1981**, *15*, 311; *Carbohydr. Res.* **1978**, *67*, C4.

Registry No. P_4VPy, 25232-41-1; cellulose, 9004-34-6; methylolcellulose, 135663-12-6.